

000 XPOISON: CROSS-CLASS ATTACKS THROUGH 001 002 CLEAN-LABEL DATA POISONING IN FINE-TUNING 003 004

005 **Anonymous authors**

006 Paper under double-blind review

007 008 ABSTRACT 009

011 As deep learning relies on huge datasets for training, poisoning attacks that pollute
012 the datasets pose a significant threat to its security. Given more models pretrained
013 on private corpora inaccessible to external parties, earlier attacks demanding ac-
014 cess to the base training datasets have their impact largely diminished, while prac-
015 tical threats focus on the finetuning stage when attackers can accurately target spe-
016 cific (intended) classes by manipulating a small subset of the dataset under their
017 control. Fortunately, attackers could potentially be exposed also thanks to the sub-
018 stantially lowered data volume: e.g., correlation between identities and provided
019 data classes poses risks to attackers. To enable stealthy poisoning, we introduce
020 XPoison that strategically performs poisoning in a *cross-class* manner. Instead
021 of directly poisoning the intended classes, a XPoison attacker only needs to pro-
022 vide dataset for unintended classes and hence hides its identity. We first propose
023 a magnitude matching strategy to more efficiently align the malicious gradients.
024 Furthermore, we estimate contradiction from clean target data and compensate
025 gradient-wise, thereby counteracting its neutralizing influence on the poisoning
026 effect. Through extensive evaluations, we demonstrate that XPoison is capable
027 of robustly reducing the recognition accuracy of targeted classes by up to 38.37%
028 during finetuning, while preserving high accuracy in poison classes.

029 1 INTRODUCTION 030

031 Deep learning has achieved remarkable successes and been widely deployed across a variety of ap-
032 plications in recent time LeCun et al. (2015). Nevertheless, the reliance of models on large-scale
033 contributed training data makes them inherently vulnerable to attacks, whereby attackers introduce
034 malicious poison to training instances to influence specific model behaviors Nelson et al. (2008).
035 While some earlier studies Geiping et al. (2021) on data poisoning have largely concentrated on
036 models trained from scratch and assumed complete access to the model and its training data, in
037 real-world settings most deployed models are pretrained on private datasets that are inaccessible to
038 external attackers. As models are tasked with increasingly complex problems, finetuning Pan &
039 Yang (2010) provides an effective mechanism for learning from previously unseen domains or re-
040 fining knowledge in existing domains; however, it also exposes a more practical window for attacks.
041 Early attacks target the specific class associated with the attacker-controlled dataset and involved
042 direct, obvious label modifications, rendering them relatively easy to detect Biggio et al. (2012).

043 To further enhance stealth and bypass detection mechanisms, attackers instead inject subtle pertur-
044 bations into the input data while leaving labels unchanged; these modified samples are known as
045 *poisons* Shafahi et al. (2018); Geiping et al. (2021). Nonetheless, this method is not sufficiently
046 stealthy: attacker-controlled finetuning subsets usually map to a few classes, making detection and
047 attribution to the poison and attacker straightforward. Thus, cross-class poisoning is a preferable
048 strategy, as it allows attackers to select misclassification targets at will instead of being limited to
049 the poisoned class, widening the threat surface.

050 Although it offers greater potential and poses higher risks, developing poison attack algorithms
051 becomes increasingly challenging, as the attack surface requires the model to learn the associa-
052 tion between modified inputs and correct labels while keeping the labels fixed. While existing
053 works Shafahi et al. (2018); Huang et al. (2020); Geiping et al. (2021) can achieve decent poisoning
effect under specific assumptions, a critical asymmetry between victims and attacks inherently lim-

054 its such attacks: in real-world model finetuning, attackers typically control only a subset of a data
 055 class, while victims may aggregate data from multiple sources and collect clean, correctly-labeled
 056 samples of that same class from other providers Russakovsky et al. (2015); Kaissis et al. (2021);
 057 Sheller et al. (2020). Such clean data contradicts cross-class poison by providing conflicting or even
 058 the exact opposite supervision signal. This raises a natural question: can attackers inject effective
 059 biases into models even when correct information of that category is simultaneously present?

060 Backdoor attacks Gu et al. (2019) can tackle this problem by learning parallel associations where
 061 a malicious shortcut to wrong mapping coexists with truthful mapping. This shortcut could be ac-
 062 tivated by the presence of either a natural Zhao & Lao (2022) or a carefully-optimized Saha et al.
 063 (2020) trigger on test-time inputs to affect specific test sample without being canceled out by clean
 064 evidence. Because the truthful mapping is still present, normal model performance of correctly clas-
 065 sifying inputs without triggers would also not be affected. However, this method loses effectiveness
 066 when such trigger isn't available during test-time: attackers may simply not have access to test data
 067 for applying triggers or the circumstances determine that they may have little control over the pres-
 068 ence of natural triggers in test data Shafahi et al. (2018). This is very likely in practical multi-source
 069 data aggregation settings like medical diagnosis or social-media content moderation, where test in-
 070 puts are directly provided by users Li et al. (2020). The core issue is that building extra pathways
 071 based on trigger only temporarily circumvents the contradictory clean information given specific
 072 conditions, but it doesn't fundamentally solve the contradiction problem. Whenever the required
 073 condition fails, the method no longer suffices. This constraint limits the practicality of clean-label
 074 backdoor attacks and makes them inefficient in this specific scenario.

075 Therefore, trigger-free cross-class poisoning presents a more suitable alternative in this setting, as
 076 this can achieve unconditional misclassification without requiring test-time trigger availability while
 077 maintaining both efficacy and covertness. Some existing such approaches like Shafahi et al. (2018);
 078 Zhu et al. (2019); Aghakhani et al. (2021) work well in transfer learning settings where a pretrained
 079 model is finetuned for downstream tasks. Their poison can to certain degree overcome contradic-
 080 tion from clean data either within frozen model knowledge or finetuning dataset. However, they
 081 heavily rely on the pretrained feature extractor and cannot work effectively in scenarios where fea-
 082 ture space changes significantly due to the large domain difference between finetuning data and
 083 pretraining data Shafahi et al. (2018). Other works like Huang et al. (2020); Geiping et al. (2021)
 084 have demonstrated promise in controlled settings and doesn't demand feature extractor remaining
 085 relatively stable, but they fundamentally assume the non-existence of clean data on target class.
 086 This assumption renders them ineffective in realistic multi-source data aggregation setting. A new
 087 method is required to overcome this challenge.

088 In this paper, we introduce XPoison, a novel attack paradigm based on gradient matching that
 089 achieves trigger-free cross-class misclassification even when contradictory clean evidence is present.
 090 We focus on the scenario of finetuning. In our setting, we assume the attackers know about the model
 091 structure.

092 XPoison employs multiclass gradient matching with two key enhancements: magnitude alignment
 093 to match both gradient direction and scale, and contradiction compensation to account for gradient
 094 interference from clean data.

095 Our contributions are:

- 096 • Formalizing trigger-free cross-class poisoning as a distinct attack category in concept
- 097 • Providing the first evaluation under realistic constraints where finetuning contains clean
 098 target information contradictory to poison and existing methods aren't suitable due to failed
 099 premises
- 100 • Identifying a practical real-world scenario that such attack threatens.
- 101 • Introducing clean interference compensation that makes attacks robust to the dilution that
 102 occurs when victims train on mixed clean-poison data

103 This defines a new attack framework for further exploration and reveals a fundamental vulnerability
 104 in real-world defense.

108 The rest of the paper is organized as follows. Section 2 briefly captures related works. Section 3
 109 presents the problem formulation in mathematical terms. Section 4 discusses details of our method.
 110 Section 5 reports the experimental results. Finally, section 6 concludes the paper.
 111

112 2 RELATED WORKS

113 2.1 MULTI-SOURCE DATA AGGREGATION

116 Multi-source data aggregation is the norm of modern ML. From massive webscraping of ImageNet
 117 to federated medical systems, many real-world ML systems inherently involve multiple untrusted
 118 data sources when collecting training data, which naturally exposes themselves to potential injec-
 119 tion of malicious data Russakovsky et al. (2015); Kaassis et al. (2021); Sheller et al. (2020). Security
 120 research in federated learning, which takes place in similar setting of distributed data sources con-
 121 verging data to a center, also shows that attacks demonstrate strong effectiveness even with a small
 122 percentage of participants being malicious Tolpegin et al. (2020). This validates the practicality of
 123 our scenario setting. Such vulnerability to malicious data sources has motivated extensive research
 124 into data poisoning attacks, which can be broadly categorized into backdoor attacks and trigger-free
 125 attacks based on their activation mechanisms.

126 2.2 BACKDOOR ATTACK

129 Backdoor attack aims to manipulate model behavior by injecting poisoned data into training and
 130 activating in test time through triggers. To increase stealthiness, clean-label backdoor attack is
 131 developed to poison data content while maintaining the correct label. For example, Saha et al.
 132 (2020) achieves misclassification by crafting poisoned images that appear similar to target-class
 133 samples in pixel space while maintaining feature representations close to trigger-patched source
 134 images. Zhao & Lao (2022) uses naturally-misclassified samples as poison; Severi et al. (2021)
 135 uses SHAP value to select the most important training samples to poison.

136 There are also works that focus on defending against such attacks or using such attacks for benign
 137 purpose. For example, He et al. (2023) trains clean model on poisoned data by isolating the poisoned
 138 samples in early training and unlearn them. The key is that stronger attacks are learned faster,
 139 which is reflected as bigger and quicker loss drop compared to normal samples Li et al. (2021) uses
 140 indiscriminate poisoning attacks to protect unauthorized data usage.

141 However, all backdoor attacks share a fundamental limitation: they require the presence of trigger
 142 during test-time to activate malicious behavior, which makes them infeasible in real-world scenarios
 143 like ours.

144 2.3 UNCONDITIONAL ATTACKS

146 To overcome the limitation of requiring test-time triggers, trigger-free attacks aim to cause un-
 147 conditional misclassification of unmodified target class through training-time manipulation alone.
 148 Shafahi et al. (2018) pioneered this direction by optimizing source-class training images to collide
 149 with target-class images in feature space, effectively associating target-class images with source-
 150 class labels. Aghakhani et al. (2021) extended this approach by crafting poisons that push target
 151 images toward a convex polytope in feature space formed by multiple poison class samples, im-
 152 proving attack transferability across different model architectures. Huang et al. (2020) formulated
 153 poisoning as a bilevel optimization problem, using expensive meta-learning to approximate the vic-
 154 tim's training process and get optimal poison optimization with unrolled gradient steps. Geiping
 155 et al. (2021) simplified this approach through gradient matching, aligning source-class gradients
 156 with target misclassification gradients and effectively decreased computational cost.

157 However, existing unconditional attacks face a critical limitation in realistic deployment scenarios:
 158 they assume the victim's training data consists minimal clean data from target class. In practice,
 159 victims typically have access to substantial amounts of clean target class data that can dilute or
 160 counteract poison effects through correct label associations. This gap between experimental as-
 161 sumptions and real-world conditions motivates our attack that remains effective even when directly-
 contradictory clean and poisoned data coexist during finetuning.

162

3 PROBLEM FORMULATION

164 In this section, we present the modeling of the task we aim to address.

166

3.1 THREAT MODEL

168 We consider a poisoning attack against deep neural networks in the finetuning stage, where attackers
169 seek to manipulate a victim model’s behavior through strategic modification of training data.170 **Attacker Capabilities:** The attacker can inject a limited number of maliciously crafted training
171 samples into the victim’s training set before the fine-tuning process begins. The attacker has no
172 control over the training procedure, model architecture, or labeling process, and must assign correct
173 labels to all injected samples (clean-label constraint).174 **Victim Model:** We assume a victim model $f_\theta : \mathcal{X} \rightarrow \mathbb{R}^C$ pretrained on a source dataset, which is
175 subsequently fine-tuned on a target dataset $\mathcal{D} = \{(x_i, y_i)\}_{i=1}^N$ where $x_i \in \mathcal{X}$ and $y_i \in \{1, 2, \dots, C\}$.177 **Attack Objective:** Given a specific target sample (x_t, y_t) from the test set, the attacker aims to
178 cause the finetuned model to misclassify x_t as one of any non- y_t classes $\mathcal{Y}_m = \{y_m^{(1)}, y_m^{(2)}, \dots, y_m^{(k)}\}$
179 where $y_t \notin \mathcal{Y}_m$, while maintaining the model’s performance on clean samples.181

3.2 MULTICLASS POISONING FRAMEWORK

183 Unlike traditional single-class approaches, we formulate a multiclass poisoning strategy that lever-
184 ages samples from multiple poison classes $\mathcal{C}_p = \{c_1, c_2, \dots, c_k\}$ where $\mathcal{C}_p \cap \{y_t\} = \emptyset$. The attacker
185 selects n_i samples from each poison class c_i , creating a poison set:

186
$$\mathcal{P} = \bigcup_{i=1}^k \mathcal{P}_i, \quad \text{where } \mathcal{P}_i = \{(x_j^{(i)}, c_i)\}_{j=1}^{n_i}. \quad (1)$$

189 The total poison budget is constrained by $|\mathcal{P}| = \sum_{i=1}^k n_i \leq \epsilon \cdot N$ for some small ϵ (typically
190 $\epsilon \leq 0.01$). Each poison sample is modified by adding an imperceptible perturbation $\delta_j^{(i)}$ subject to
191 the constraint $\|\delta_j^{(i)}\|_\infty \leq \xi$ for some small ξ , yielding poisoned samples $\tilde{x}_j^{(i)} = x_j^{(i)} + \delta_j^{(i)}$.
192194

4 METHOD

196 In this section, we begin by detailing the XPoison framework and subsequently extend it to address
197 the multi-class scenario.199

4.1 ENHANCED GRADIENT MATCHING

201 Vanilla gradient matching Geiping et al. (2021) aims to cause unconditional misclassification by
202 matching the gradient of selected poisoned-class samples with that of target-class instances paired
203 with poisoned-class label. Given a target image x_t with true label y_t and intended malicious label
204 y_m , the attack optimizes poison samples $\{x_p^{(i)}\}$ with correct labels $\{y_p^{(i)}\}$ to minimize:

205
$$\mathcal{L}_{\text{direction}} = - \sum_l \langle \nabla_{\theta_l} \mathcal{L}(f_\theta(x_t), y_m), \nabla_{\theta_l} \mathcal{L}(f_\theta(x_p), y_p) \rangle, \quad (2)$$

208 where θ_l represents parameters of layer l , and the objective maximizes alignment between target and
209 poison gradients.210 While directional alignment ensures the poisoned samples point to the same directions as target
211 gradients, vanilla gradient matching suffers from two critical limitations. First, gradients aligning in
212 direction may still differ significantly in magnitude, leading to potentially suboptimal optimization
213 step sizes and consequently poor convergence to attack objectives. Second, during finetuning, clean
214 samples from target class generate contradictory gradients that directly counters the poison signal,
215 which significantly reduces the poison effectiveness as the vanilla approach lacks sufficient strength
to overcome the contradiction and achieve effectiveness. As formulated in Eqn. 3, during victim

216 finetuning, the actual gradient experienced by the model combines poison effects with clean data
217 interference:

$$218 \quad \mathbf{g}_{\text{total}} = \mathbf{g}_{\text{poison}} + \mathbf{g}_{\text{clean}}. \quad (3)$$

219 Vanilla gradient matching optimizes for $\mathbf{g}_{\text{poison}} \approx \mathbf{g}_{\text{target}}$, but the actual optimization direction be-
220 comes $\mathbf{g}_{\text{poison}} + \mathbf{g}_{\text{clean}}$. This is why poison gradient needs to be enhanced so that clean gradient
221 cannot effectively push toward correct classification.

222 To address the limitations mentioned, we propose multiple enhancements as solution:

224

- 225 • Magnitude alignment: Explicitly matching the poisoned samples’ magnitude with target
226 samples’ magnitude in addition to the existing directional alignment. This ensures that
227 poisoned samples not only optimize in the right direction but also update in appropriate
228 strength to overcome potential contradiction from clean samples.
- 229 • Clean interference compensation: Estimating the potential impact of clean target data on
230 poison gradient by projection for compensation. This ensures the poison becomes more
231 robust to clean data interference in actual finetuning since clean effects are already approx-
232 imated in optimization.

233 Our enhanced objective function becomes:

$$234 \quad \mathcal{L}_{\text{enhanced}} = \alpha \cdot \mathcal{L}_{\text{direction}}(\mathbf{g}_t^*, \mathbf{g}_p) + \beta \cdot \mathcal{L}_{\text{magnitude}}(\mathbf{g}_t^*, \mathbf{g}_p), \quad (4)$$

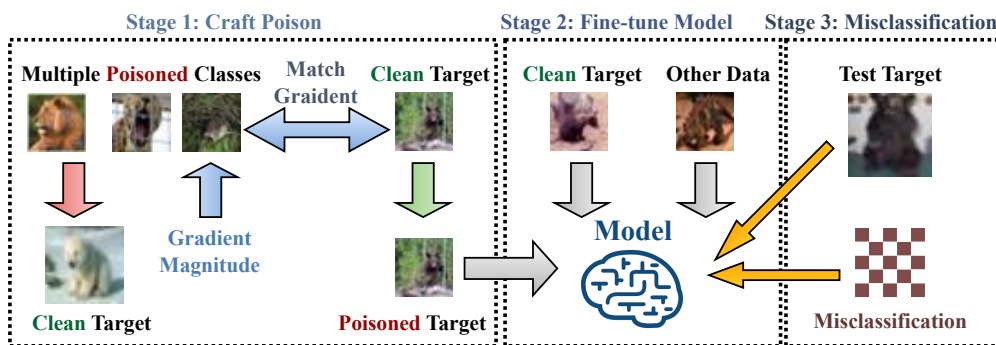
235 where \mathbf{g}_t^* represents the **compensated target gradient** and \mathbf{g}_p represents poison gradients. To
236 compute compensation, we estimate clean interference $\hat{\mathbf{g}}_{\text{clean}}$ using proxy clean samples and subtract
237 that influence from the target gradient:

$$238 \quad \mathbf{g}_t^* = \mathbf{g}_t - \gamma \cdot \text{proj}_{\hat{\mathbf{g}}_{\text{clean}}}(\mathbf{g}_t), \quad (5)$$

240 where γ controls compensation strength and $\text{proj}_{\hat{\mathbf{g}}_{\text{clean}}}(\mathbf{g}_t)$ represents the projection of target gra-
241 dients onto the clean interference direction. Due to the significant difference between layers on
242 gradient scales and feature-extraction roles, we apply compensation independently to each layer l
243 for layer-specific projection coefficients:

$$244 \quad \mathbf{g}_{t,l}^* = \mathbf{g}_{t,l} - \gamma \cdot \frac{\langle \mathbf{g}_{t,l}, \hat{\mathbf{g}}_{\text{clean},l} \rangle}{\| \hat{\mathbf{g}}_{\text{clean},l} \|^2} \hat{\mathbf{g}}_{\text{clean},l}. \quad (6)$$

246 This removes the component of target gradients that aligns with expected clean interference while
247 preserving magnitude through renormalization, thereby achieving more robust poison against con-
248 tradictory clean signal. Note that since this is approximation in experimental conditions, samples
249 are randomly selected from the target class in finetuning dataset. Within real-world scenarios, this
250 should be done by sampling representative target class data from external data sources since attack-
251 ers may not have access to target class data actually used for finetuning. Building on the com-
252 pensated target gradients, we add explicit magnitude matching in the form of ratio between \mathbf{g}_p and \mathbf{g}_t^*



254

255

256

257

258

259

260

261

262

263

264

265

266

267

268

269

Figure 1: An overview of our poisoning process. Stage 1: Poison samples from multiple classes are crafted to match gradients with a clean target image, enhanced with magnitude alignment and clean interference compensation. Stage 2: The victim model is finetuned on a dataset containing both poisoned samples and clean data. Stage 3: At test time, the target class image is misclassified, demonstrating successful cross-class attack. .

270 to encourage poisoned gradient to either match or succeed the target gradient for greater poison
271 strength:

$$272 \quad \mathcal{L}_{\text{magnitude}} = -\log \left(\frac{\|\mathbf{g}_p\|_2}{\|\mathbf{g}_t^*\|_2 + \epsilon} \right). \quad (7)$$

275 The logarithmic formulation provides several advantages: it naturally handles the vastly different
276 gradient scales across model layers by compressing the value range for consistent processing, pre-
277 vents optimization instability by bounding extreme magnitude ratios and providing smooth deriva-
278 tives that avoid sudden jumps during gradient descent, and ensures balanced treatment of both under-
279 magnitude and over-magnitude scenarios for more stable optimization.

281 4.2 MULTI-CLASS POISONING ENHANCEMENT

283 To further boost the attack effectiveness, we extend our enhanced framework to **multi-class poison-**
284 **ing**, where poisoned samples are distributed across multiple classes instead of one.

285 Given a set of poison classes $\mathcal{C}_p = \{c_1, c_2, \dots, c_k\}$, we distribute the poison budget B across all
286 classes:

$$287 \quad B_i = \left\lceil \frac{B}{|\mathcal{C}_p|} \right\rceil \text{ for each class } c_i \in \mathcal{C}_p. \quad (8)$$

290 We also compute target gradients by averaging across all intended classes rather than using a single
291 intended class:

$$292 \quad \mathbf{g}_t = \frac{1}{|\mathcal{C}_p|} \sum_{c_i \in \mathcal{C}_p} \nabla_{\theta} \mathcal{L}(f_{\theta}(x_t), c_i). \quad (9)$$

295 This averaged gradient represents the optimization direction toward the centroid of the poisoned
296 class space, providing a potentially more robust and generalizable attack target. Also, the multi-
297 class approach integrates seamlessly with our existing enhancement framework. Clean gradients are
298 estimated independently for each poison class and averaged:

$$299 \quad \hat{\mathbf{g}}_{\text{clean}} = \frac{1}{|\mathcal{C}_p|} \sum_{c_i \in \mathcal{C}_p} \hat{\mathbf{g}}_{\text{clean}, c_i}. \quad (10)$$

303 **Algorithm 1** Enhanced Gradient Matching with Dual Compensation (Multi-class)

305 **Require:** Target (x_t, y_t) , Intended classes $\{y_m^{(j)}\}$, Poison set $\{(x_p^{(i)}, y_p^{(i)})\}$, Model f_{θ}
306 **Require:** Parameters: α, β, γ , learning rate η , iterations T
307 1: Estimate clean interference: $\hat{\mathbf{g}}_{\text{clean}} \leftarrow \text{EstimateCleanGradients}(x_t, y_t)$
308 2: Initialize poison perturbations: $\Delta^{(i)} \leftarrow \mathbf{0}$
309 3: **for** $t = 1$ to T **do**
310 4: Apply perturbations: $x_p'^{(i)} \leftarrow x_p^{(i)} + \Delta^{(i)}$
311 5: **Multi-class target gradient:**
312 6: $\mathbf{g}_t \leftarrow \frac{1}{|\{y_m^{(j)}\}|} \sum_j \nabla_{\theta} \mathcal{L}(f_{\theta}(x_t), y_m^{(j)})$
313 7: Compensate target gradient: $\mathbf{g}_t^* \leftarrow \text{CompensateGradient}(\mathbf{g}_t, \hat{\mathbf{g}}_{\text{clean}}, \gamma)$
314 8: **for** each poison i **do**
315 9: Compute poison gradient: $\mathbf{g}_p^{(i)} \leftarrow \nabla_{\theta} \mathcal{L}(f_{\theta}(x_p'^{(i)}), y_p^{(i)})$
316 10: Compute direction loss: $\mathcal{L}_{\text{dir}}^{(i)} \leftarrow -\langle \mathbf{g}_t^*, \mathbf{g}_p^{(i)} \rangle / \|\mathbf{g}_t^*\|$
317 11: Compute magnitude loss: $\mathcal{L}_{\text{mag}}^{(i)} \leftarrow -\log(\|\mathbf{g}_p^{(i)}\| / (\|\mathbf{g}_t^*\| + \epsilon))$
318 12: Combined loss: $\mathcal{L}_{\text{enhanced}}^{(i)} \leftarrow \alpha \cdot \mathcal{L}_{\text{dir}}^{(i)} + \beta \cdot \mathcal{L}_{\text{mag}}^{(i)}$
319 13: **end for**
320 14: Update perturbations: $\Delta^{(i)} \leftarrow \Delta^{(i)} - \eta \nabla_{\Delta} \mathcal{L}_{\text{enhanced}}^{(i)}$
321 15: Project perturbations: $\Delta^{(i)} \leftarrow \text{Proj}_{\epsilon}(\Delta^{(i)})$
322 16: **end for**
323 17: **return** $\{x_p^{(i)} + \Delta^{(i)}\}$



Figure 2: An image example of before and after applying the poison.

324
325
326
327
328
329
330
331
332
333
334
335
336
337
338
339
340
341
342
343
344
345
346
347
348
349
350
351
352
353
354
355
356
357
358
359
360
361
362
363
364
365
366
367
368
369
370
371
372
373
374
375
376
377

It is later applied to the averaged target gradient:

$$\mathbf{g}_t^* = \mathbf{g}_t - \gamma \cdot \text{proj}_{\hat{\mathbf{g}}_{\text{clean}}}(\mathbf{g}_t). \quad (11)$$

The complete algorithm detail can be seen in Algorithm 1. Figure 2 presents an example image of before and after applying the poison.

5 EXPERIMENT

In this section, we begin by presenting the experiment setup, followed by a comprehensive evaluation of XPoison.

5.1 EXPERIMENT SETUP

For fair comparison with existing baselines, we evaluate on ImageNet-pretrained ResNet18 finetuned on CIFAR-100. This represents a realistic transfer learning scenario where attackers target models adapted to new domains or improved on old domains. This setup also highlights the advantages of our gradient-based enhancements even in favorable conditions for feature-based methods.

All our experiments are conducted on two nvidia A5000 GPUs. We set the perturbation budget to 8/255, which means maximum 8 intensity levels are allowed to be changed out of all possible values, making poisoned images visually imperceptible to humans but effectively toxic to model, balancing attack stealthiness with effectiveness. The finetuning learning rate is set to 0.1, selected empirically for optimal performance. Other hyperparameters are kept as default.

We also investigate how pretrained feature representations as clean frozen knowledge affect poisoning transferability by comparing attacks on classes with and without ImageNet overlap. This may better improve the poison effectiveness and isolate the feasibility of poison countering fresh clean target data for finetuning. While pretrained knowledge is absent, poisoned classes include dinosaur, plain, rocket, forest, mountain, sea, shrew, caterpillar, possum, and baby. Target class is cloud. While pretrained knowledge is present, poisoned classes include lion, leopard, tiger, bicycle, motorcycle, shark, whale, spider, fox and elephant. Target class is bear. Note that these experimental configurations involve manual class selection and is an imperfect simulation to the strict domain boundaries typically enforced in real-world deployment.

While design-wise target image is optimized to be misclassified as any of the poisoned classes, in reality, it is acceptable for it to be misclassified as any non-target class.

5.2 OVERALL PERFORMANCE

Table 1 shows the comparison between our method and the baseline methods. Compared with clean baseline where no poison is introduced in finetuning, feature-based methods like Poison Frogs Shafahi et al. (2018) and Bullseye Aghakhani et al. (2021), in which poisoned samples are optimized to approach target samples in feature space, have achieved reasonable attack success that reduces target class accuracies by 28.27% and 9.08%, respectively. However, such effectiveness comes with a heavy cost as they are not stealthy enough and cannot maintain decent accuracy on poison class, making them inappropriate for real-world deployment in this scenario. While vanilla gradient matching Geiping et al. (2021) preserves poison class accuracy, it only reduces target class accuracy

378 by 8.07%, indicating limited attack effectiveness. In contrast, our method achieves a reduction of
 379 38.37%, exceeding the feature-based methods while mostly preserving recognition ability on poison
 380 class with a small drop of 2.8%. This indicates the effectiveness and stealthiness of our method.
 381
 382

383 Table 1: Performance comparison with baselines

384 Method	385 Poison Class Acc (%)	386 Target Correct (%)
Clean	88.00	88.88
Poison Frogs	24.00	60.61
Bullseye	12.00	79.80
Gradient matching	83.30	80.81
Ours	85.20	50.51

390
 391 5.3 IN-DEPTH ANALYSIS
 392

393 As shown in Table 2, the best result among all different poison class numbers was achieved in
 394 10 poisoned classes with a drop of 38.37% on target classification rate. While having only one
 395 poisoned class, classification rate on poisoned class cannot be maintained well and dropped to 35%
 396 while demonstrating suboptimal attack effectiveness. This is likely due to excessive pixel change,
 397 which achieved small target misclassification rate at the cost of a complete destruction of poison
 398 class recognition. As poison becomes distributed in multiple classes, target recognition linearly
 399 drops as poisoned class number increases while preserving a decent level of poison class recognition
 400 capability. Due to limited computational resources, we limit the class number within 10.
 401

402 Table 2: Performance comparison across different numbers of poison classes

403 Classes	404 Poison Class Acc (%)	405 Target Correct (%)
Clean	88.00	88.88
1	35.00	83.84
3	87.00	83.84
5	88.00	82.83
7	85.57	68.69
10	85.20	50.51

410 We also tested when selected classes have no overlap with the pretraining dataset so that the model
 411 has no clean frozen knowledge on them. As shown in Table 3, single poison class achieves only
 412 43.00% poison class accuracy despite having a decent 71.72% target correct rate, indicating poor
 413 attack stealthiness. After entering multi-class poisoning, poison class accuracy gradually drops from
 414 little poison effect in 3 classes to 76.77% with 5 and 7 classes, while in the end slightly increasing
 415 back to 80.81% with 10 classes. This U-shaped pattern in target accuracy differs from the linear trend
 416 observed in the case with pretrained knowledge, suggesting that the model’s adaptation dynamics
 417 vary substantially when learning entirely new classes versus refining existing ones. The sustained
 418 high poison class accuracy, combined with reasonable attack success rate, indicates that our attack
 419 remains effective even without pretrained knowledge present.
 420

421 Table 3: Comparison across different numbers of poison classes without pretrained knowledge

422 Classes	423 Poison Class Acc (%)	424 Target Correct (%)
Clean	88.00	88.88
Best	85.20	50.51
1	43.00	71.72
3	95.67	88.89
5	91.00	76.77
7	88.14	76.77
10	79.50	80.81

430 We also examined the influence of different target class on the attack performance by randomly
 431 selecting poison classes from the 10 classes with pretrained knowledge as target. As shown in

432 Table 4, our method demonstrates consistent performance across different target classes, with poison
 433 class accuracy remaining high (75.60-81.60%) and averaging 78.94%. The target correct rates show
 434 substantial variation across different target classes, ranging from 55.56% to 73.74% with an average
 435 of 67.68%. Target class 88 achieves the strongest attack success with only 55.56% of target samples
 436 correctly classified, while maintaining 78.10% poison class accuracy. Target class 43 shows the
 437 highest poison class accuracy with 81.60%, but its target correct is at 70.71%, slightly lower than
 438 class 88. Overall, this demonstrates that our multiclass gradient matching approach can maintain
 439 excellent poison stealthiness and effectiveness regardless of the specific target class chosen.

440

441

Table 4: Attack performance across different target classes

Target Class	Poison Class Acc (%)	Target Correct (%)
31	79.60	73.74
42	75.60	65.66
43	81.60	70.71
73	79.80	72.73
88	78.10	55.56
Average*	78.94	67.68

442

450 Table 5 shows our ablation study on enhancement components. We use the best result under 10
 451 poison classes and measure accuracies under different component weight configurations at the same
 452 step for fair comparison. β represents the weight of magnitude-matching, while γ represents the
 453 weight of clean compensation. Compared with the baseline of vanilla implementation where both
 454 weights are zero, the individual enhancement components demonstrate a modest improvement, with
 455 a maximum of 5.05% reduction in target class accuracies. When both are combined, they further
 456 result in a substantial 30.30% decrease compared with baseline, confirming the effectiveness of our
 457 proposed method.

458

499

Table 5: Ablation study

β	γ	Poison Class Acc (%)	Target Correct (%)
1	1	85.20	50.51
1	0	77.40	77.75
0	1	80.60	75.76
0	0	83.30	80.81

500

501

6 CONCLUSION

502

503 In this work, we have addressed a critical gap in data poisoning research by examining cross-class
 504 attacks under realistic finetuning scenarios where victims possess clean target samples that directly
 505 contradict attacker-controlled poisons. The demonstrated effectiveness of trigger-free cross-class
 506 poisoning under realistic constraints has significant implications for deployed machine learning
 507 systems. Organizations that aggregate finetuning data from multiple sources face previously underesti-
 508 mated vulnerabilities. Even when defenders possess substantial amounts of clean data, sophisticated
 509 attackers can still manipulate model behavior through carefully crafted poison samples distributed
 510 across a small amount of classes. The formalization of trigger-free cross-class poisoning as a dis-
 511 tinct threat category provides a foundation for future defensive research and helps practitioners better
 512 assess risks in their ML pipelines.

513

514

515 Our evaluation focuses primarily on image classification tasks using CIFAR-100 in transfer learning
 516 scenarios. Future work should extend these findings to other domains, larger-scale datasets, and dif-
 517 ferent model architectures. Additionally, investigating defensive mechanisms specifically designed
 518 to handle mixed clean-poison scenarios or cross-class manipulation represents an important research
 519 direction.

520

521

522

486 **Ethics Statement:** This work adheres to the ICLR Code of Ethics and presents data poisoning
 487 attacks for research and defensive purposes to advance understanding of ML vulnerabilities and
 488 enable better defenses. We do not advocate for malicious use of presented methods.

489 **Reproducibility:** To ensure reproducibility, we will release the complete source code for verifica-
 490 tion upon acceptance.

492 **LLM usage:** This paper used LLM for aiding writing polishing. LLM was not involved in the
 493 idealization, method conceptualization, or experimental design. All research concepts and analyses
 494 were developed and conducted by the authors.

496 REFERENCES

498 Hojjat Aghakhani, Dongyu Meng, Yu-Xiang Wang, Christopher Kruegel, and Giovanni Vigna.
 499 Bullseye Polytope: A Scalable Clean-Label Poisoning Attack with Improved Transferability. In
 500 *Proc. of 6th IEEE EuroS&P*, pp. 159–178, 2021.

501 Battista Biggio, Blaine Nelson, and Pavel Laskov. Poisoning Attacks Against Support Vector Ma-
 502 chines. In *Proc. of the 29th ICML*, pp. 1807–1814, 2012.

503 Jonas Geiping, Liam Fowl, W. Ronny Huang, Wojciech Czaja, Gavin Taylor, Michael Moeller, and
 504 Tom Goldstein. Witches’ Brew: Industrial Scale Data Poisoning via Gradient Matching, 2021.
 505 URL <https://arxiv.org/abs/2009.02276>.

507 Tianyu Gu, Brendan Dolan-Gavitt, and Siddharth Garg. BadNets: Identifying Vulnerabilities in
 508 the Machine Learning Model Supply Chain, 2019. URL <https://arxiv.org/abs/1708.06733>.

510 Hao He, Kaiwen Zha, and Dina Katabi. Indiscriminate Poisoning Attacks on Unsupervised Con-
 511 trastive Learning, 2023. URL <https://arxiv.org/abs/2202.11202>.

513 W. Ronny Huang, Jonas Geiping, Liam Fowl, Gavin Taylor, and Tom Goldstein. MetaPoison:
 514 Practical General-purpose Clean-label Data Poisoning. In *Proc. of the 34th NeurIPS*, 2020.

516 Georgios Kaassis, Alexander Ziller, Jonathan Passerat-Palmbach, Théo Ryffel, Dmitrii Usvin, An-
 517 drew Trask, Ionésio Lima Jr, Jason Mancuso, Friederike Jungmann, Marc-Matthias Steinborn,
 518 et al. End-to-End Privacy Preserving Deep Learning on Multi-institutional Medical Imaging.
 519 *Nature Machine Intelligence*, 3(6):473–484, 2021.

520 Yann LeCun, Yoshua Bengio, and Geoffrey Hinton. Deep Learning. *Nature*, 521(7553):436–444,
 521 2015. doi: 10.1038/nature14539.

522 Tian Li, Anit Kumar Sahu, Ameet Talwalkar, and Virginia Smith. Federated learning: Challenges,
 523 methods, and future directions. *IEEE Signal Processing Magazine*, 37(3):50–60, 2020.

525 Yige Li, Xixiang Lyu, Nodens Koren, Lingjuan Lyu, Bo Li, and Xingjun Ma. Anti-backdoor Learn-
 526 ing: Training Clean Models on Poisoned Data. *Proc. of the 35th NeurIPS*, 34:14900–14912,
 527 2021.

528 Blaine Nelson, Marco Barreno, Fuching Jack Chi, Anthony D. Joseph, Benjamin I.P. Rubinstein,
 529 Udam Saini, Charles Sutton, and Kai Xia. Exploiting Machine Learning to Subvert Your Spam
 530 Filter. In *Proc. of the 1st USENIX Workshop on Large-Scale Exploits and Emergent Threats*,
 531 2008.

533 Sinno Jialin Pan and Qiang Yang. A Survey on Transfer Learning. *IEEE Transactions on Knowledge
 534 and Data Engineering*, 22(10):1345–1359, 2010. doi: 10.1109/TKDE.2009.191.

535 Olga Russakovsky, Jia Deng, Hao Su, Jonathan Krause, Sanjeev Satheesh, Sean Ma, Zhiheng
 536 Huang, Andrej Karpathy, Aditya Khosla, Michael Bernstein, et al. Imagenet Large Scale Visual
 537 Recognition Challenge. *International Journal of Computer Vision*, 115(3):211–252, 2015.

539 Aniruddha Saha, Akshayvarun Subramanya, and Hamed Pirsiavash. Hidden Trigger Backdoor At-
 540 tacks. In *Proc. of the 34th AAAI*, volume 34, pp. 11957–11965, 2020.

540 Giorgio Severi, Jim Meyer, Scott Coull, and Alina Oprea. Explanation-Guided Backdoor Poisoning
541 Attacks Against Malware Classifiers. In *Proc. of 30th USENIX Security Symposium*, pp. 1487–
542 1504, 2021. ISBN 978-1-939133-24-3.

543 Ali Shafahi, W Ronny Huang, Mahyar Najibi, Octavian Suciu, Christoph Studer, Tudor Dumitras,
544 and Tom Goldstein. Poison Frogs! Targeted Clean-Label Poisoning Attacks on Neural Networks.
545 In *Proc. of the 32nd NeurIPS*, 2018.

546 Micah J. Sheller, Brandon Edwards, G. Anthony Reina, Jason Martin, Sarthak Pati, Aikaterini
547 Kotrotsou, Mikhail Milchenko, Weilin Xu, Daniel Marcus, Rivka R. Colen, and Spyridon Bakas.
548 Federated Learning in Medicine: Facilitating Multi-Institutional Collaborations Without Sharing
549 Patient Data. *Scientific Reports*, 2020.

550 Vale Tolpegin, Stacey Truex, Mehmet Emre Gursoy, and Ling Liu. Data Poisoning Attacks Against
551 Federated Learning Systems. In *Proc. of the 25th ESORICS*, pp. 480–501, 2020.

552 Bingyin Zhao and Yingjie Lao. CLPA: Clean-Label Poisoning Availability Attacks Using Genera-
553 tive Adversarial Nets. In *Proc. of the 36th AAAI*, volume 36, pp. 9162–9170, 2022.

554 Chen Zhu, W Ronny Huang, Hengduo Li, Gavin Taylor, Christoph Studer, and Tom Goldstein.
555 Transferable Clean-Label Poisoning Attacks on Deep Neural Nets. In *Proc. of the 36th PMLR*,
556 pp. 7614–7623, 2019.

557
558
559
560
561
562
563
564
565
566
567
568
569
570
571
572
573
574
575
576
577
578
579
580
581
582
583
584
585
586
587
588
589
590
591
592
593